Light-Scattering Study of Kinetics of Spinodal Decomposition in a Polymer Solution

Jyotsana Lal and Rama Bansil*

Center for Polymer Studies and Department of Physics, Boston University, Boston, Massachusetts 02215

Received January 11, 1990; Revised Manuscript Received June 19, 1990

ABSTRACT: Small-angle light scattering was used to measure the time evolution of the structure factor $S(k,t)$ at various times t after quenching polystyrene-cyclohexane (PS-CH) solutions to a temperature below the spinodal temperature. Qualitatively, we observe the usual features of spinodal decomposition kinetics. The initial part of the phase-separation process shows an exponential increase in intensity. An analysis in terms of the linear Cahn-Hilliard theory was made to determine the extrapolated growth rate at zero time and hence the initial diffusion constant. By comparing the initial growth rates for two different molecular weights of PS, we find evidence of Zimm dynamics in these dilute solutions. The characteristic domain size shows power law growth with an exponent ranging between 0.4 and 0.5. However, the growth of intensity at the maximum of the structure factor does not exhibit any extensive region of power law growth; i.e., the exponent varies with time. The later stages of the structure factor data appear to collapse when rescaled with appropriate units of length and time. From a detailed analysis of the k-dependence of the scaled structure factor, we present some possible explanations of the interesting morphology occurring in the intermediate stages. Our results are discussed in terms of current theory and compared with the results seen in polymer blends and simple liquid mixtures.

Introduction

The kinetics of phase separation via the process of spinodal decomposition has been the subject of extensive theoretical and experimental study in widely different systems[1] such as binary liquids, high molecular weight polymer blends, inorganic glasses, and metallic alloys. Despite numerous differences at the molecular levels, many qualitative and quantitative similarities seem to be common among them. Several studies[2-7] have shown that the early stages of spinodal decomposition in polymer blends are consistent with the predictions of the linear model originally formulated by Cahn and Hilliard[8] and modified by Cook[9] to include the effects of thermal noise. The Cahn-Hilliard-Cook model (referred as CHC in this paper) has been adapted for polymer blends by de Gennes,[10] Pincus,[11] and Binder.[12] The linear (CHC) theory neglects coupling between fluctuations of different sizes, and this approximation is valid for the early stages of spinodal decomposition in polymer blends where mean-field description works quite well.

In contrast to the situation with polymer blends, relatively little work has been done on the kinetics of phase separation in polymer solutions. Smolders et al.[13] studied the kinetics of spinodal decomposition of PPO in caprolactam by measuring the time development of the turbidity following a quench into the spinodal region and interpreted their results in terms of the Cahn-Hilliard theory. However, the time evolution of the structure factor $S(k,t)$ was not measured. In view of the recent advances in the understanding of spinodal decomposition, we have undertaken a detailed study of the spinodal decomposition kinetics in solutions of polystyrene in cyclohexane (PS-CH). The equilibrium phase diagrams for various molecular weights of polystyrene in cyclohexane and the critical behavior are well-known.[14-17,19] In this paper we present results of a small-angle light-scattering (SALS) study of spinodal decomposition in two PS-CH samples differing in molecular weight. We find that, although there are qualitative similarities, many of the features of spinodal decomposition kinetics differ from those reported for[20,21] simple fluid systems and[2-7] polymer blends.

Experimental Methods

(a) Equilibrium Measurements. Solutions of polystyrene (Polysciences; $M_w = 2.33 \times 10^5$, $M_w/M_n = 1.06$, for sample 1 and $M_w = 2.80 \times 10^6$, $M_w/M_n = 1.08$, for sample 2) in cyclohexane (Fisher) were sealed in reentrant quartz cells (path lengths 0.1 and 0.2 mm for samples 1 and 2, respectively). The concentrations of the two samples were 7% and 1% (w/v), respectively. The solution was filtered by a 5-μm Millipore filter. Sample 1 is very close to critical composition as estimated from the data for polystyrene of $M_w = 2.0 \times 10^5$ by using appropriate M_w scaling.[15] This was also verified experimentally by estimating the equilibrium coexistence curve by measuring the volume ratios of the two separated phases produced by leaving the 7% PS by weight sample for 24-48 h at the desired temperature. Sample 2 is perhaps a little further from criticality, since the critical composition for $M_w = 1.56 \times 10^6$ is reported as a 0.03 volume fraction of polystyrene.[17] However, in view of the extremely flat coexistence curve in high molecular weight polymer solutions, critical effects may still be important. It should be noted that both samples are in the range just around the overlap concentration, ρ^*, since $\rho^* \sim 0.06$ g/mL for sample 1 and ~ 0.017 g/mL for sample 2, using the relation $\rho^* = (\sqrt{2}R_g)^{-3} M_w/N_A$, where N_A is Avogadro's number and R_g the radius of gyration of the polymer.[18]

Two independent estimates of the spinodal temperature, T_s, were made by measuring the scattered intensity, I, and the diffusion constant, D, at several temperatures in the one-phase region by quasi-elastic light scattering (QELS). The QELS measurements were made on a 72-channel Langley Ford 1096 correlator with an argon ion laser (power 620 mW) at a scattering angle of 90°. The diffusion constant was measured from the decay of the intensity autocorrelation function, $\sim e^{(-Dk^2t)}$, using a second-order cumulant analysis. The scattered intensity was obtained from the run duration and the total number of photocounts. QELS techniques have been used by several investigators[16,22] to determine T_s. Since PS-CH solution behaves as an Ising system[22] near the critical point and the pseudospinodal curve, the divergence of scattered intensity, I, and the vanishing of the diffusion constant, D, as T approaches T_s can be used to estimate T_s. By plotting $(I/T)^{-1/\gamma}$ versus $T(\gamma = 1.22)$ and extrapolating to zero, one obtains T_s. Similarly, plotting $(D/T)^{1/\nu}$ versus $T(\nu = 0.62)$ and extrapolating to zero also provides T_s. Results for sample 1 are shown in parts a and b of Figure 1, and the extrapolation gives $T_s = 298 \pm 0.25$ K. Similar analysis for sample 2 gives $T_s = 304.1 \pm 0.15$ K. It should be pointed out that, although a spinodal or pseudospinodal temperature can be defined

0024-9297/91/2224-0290$02.50/0

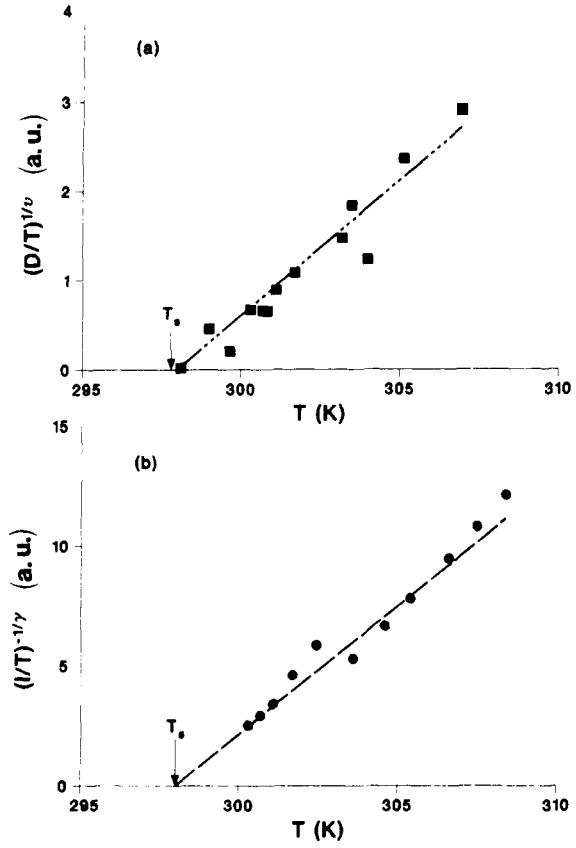

Figure 1. Results of QELS measurements in the one-phase region on sample 1 at different temperatures: (a) By plotting $(D/T)^{1/\nu}$ versus T (ν = 0.62) and extrapolating to zero, one obtains T_s as discussed in the text. (b) Similarly plotting $(I/T)^{-1/\gamma}$ versus T (γ = 1.22) and extrapolating to zero also provides T_s. Note that units and scale factors are left out in these plots.

by these extrapolations, the concept of a sharp spinodal line is strictly valid only in the mean-field description of infinite-range interactions. However, for our purposes it is not necessary to define a sharp spinodal line. T_s merely represents a gradual transition from the nucleation mechanism to the spinodal decomposition mechanism.

The results of the equilibrium measurements are also in agreement with the critical behavior of PS in CH reported by Perzynski et al.[19] From the equilibrium study of polymer interactions in a poor solvent using light-scattering techniques for PS in CH, they found the scaling relations

$$c_c = 6.8M_w^{-0.38\pm0.01} \quad (1)$$

$$10^3/T_c\,(\mathrm{K}) = 3.256(1 + (14.6 \pm 0.2)/M_w^{1/2}) \quad (2)$$

where c_c is the critical solution concentration in grams per milliliter. These relations give T_c = 298.1 and 304.5 K and the critical concentrations c_c = 0.062 and 0.024 g/mL for samples 1 and 2, respectively. These results suggest that both samples are slightly off critical.

(b) Kinetic Measurements. The experimental procedure for measurement of spinodal decomposition kinetics involved mixing the PS-CH solution at 313 K (above the critical and Θ temperature) and then transferring the sample to a temperature-controlled bath maintained at the desired final temperature in the unstable, spinodal region. We found that for all cases the sample equilibrated to the quench temperature in 10 s. The accuracy of temperature control was ±0.01 K.

The kinetics of phase separation was studied by SALS using the conical lens[23] technique to measure the angular dependence of the scattered light intensity at various times after the sample was quenched to a temperature in the two-phase region. The conical lens focuses light scattered at a given angle θ to a single point along the optic axis. Thus, by moving a photodiode

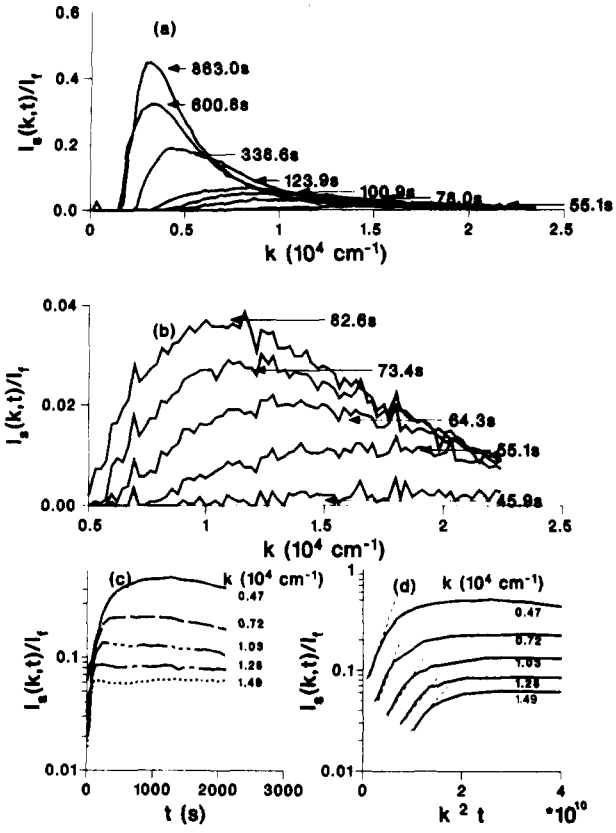

Figure 2. Typical SALS results showing the time evolution of the scattered intensity following a quench in the spinodal region. The data shown is for sample 2 with T_q = 303.85 K: (a) The scattering profile over the entire duration of the experiment. (b) Early stages of time evolution of the structure factor. In (a) and (b) the background intensity has been subtracted. (c) The scattered intensity without background subtraction as a function of time for selected values of k. (d) The initial part of the same data as in (c) versus k^2t. From such a plot we obtain the initial slope, $R(k)$.

mounted on a computer-controlled stage, we measured the angular dependence of scattered light intensity $I_s(k,t)$ (proportional to the dynamic structure factor $S(k,t)$), at a fixed time t after the quench. Here $k = 4\pi n \sin(\theta/2)/\lambda$ is the scattering vector where λ = 633 nm is the vacuum wavelength and n = 1.43 is the refractive index of the solution. The sweep time (5 s) was small compared to the collapse time of the ring (~500 s). The angular resolution was ±0.35°, and the angular range corresponds to $0.30 \times 10^4 < k < 2.2 \times 10^4$ cm^{-1}. The conical lens system was calibrated by using a diffraction grating mounted on a reentrant cell filled with cyclohexane and of exactly the same dimensions as those used for the PS-CH samples. The main advantage of the conical lens method lies in the fact that it performs an azimuthal integration of the intensity of the scattered light at a fixed angle θ, and this leads to much higher signal to noise ratios than possible with other techniques such as multiangle, multidetector spectrometers.

Results and Discussion

Upon quenching the sample to a temperature below the spinodal, we observe diffuse, weak scattering, which sharpens into a well-defined diffraction ring as time proceeds. As the process of phase separation continues, this ring grows more intense and its diameter decreases. These qualitative observations are characteristic of a spinodal decomposition process, with the diameter of the ring related to the characteristic wave vector at which the growth is most pronounced.

Figure 2a shows a typical plot of $I_s(k,t)/I_t$, the scattered intensity normalized by the transmitted intensity of the laser beam, versus the magnitude of scattering vector, k,

at different times after the sample 2 was quenched to 303.85 K. At earlier times the composition fluctuations are too small to be measured. The ring initially appears at large k, and with time the peak of the ring shifts into smaller k and the intensity of the ring grows. The peak position, k_m, continues to shift in until it overlaps with the forward beam and then cannot be detected. Note that the background scattering, $I_s(k,t = 0)$, has been subtracted, and to correct for effects of multiple scattering, the scattered intensity is normalized by the transmitted intensity, I_f.[21] Figure 2b shows mainly the early stages of the same data. Note that, although the peak is shifting in, on the high k end the curves for different times appear to be approaching a common intersection point. Such a behavior is one of the characteristic features of the linear CHC model.

Figure 2c shows intensity as a function of t at selected values of k for the same data as in Figure 2a. We note a very rapid rise of intensity at early times followed by a slower growth at later times. For each of the k values the intensity reaches its maximum value at some time and then decreases, which is consistent with late-stage coarsening phenomena.[21] Also the time at which this maximum is reached is larger for smaller k's (i.e., larger size) as expected for the growth of phase-separating domains. To investigate further the rapid increase in the intensity at very early times, we have plotted a part of the same data versus k^2t in Figure 2d. The initial growth appears to be exponential, suggesting that the CHC model may be applicable at very early stages. However, the peak position appears to be shifting in from the very first measurement (cf. Figure 2b). Thus, unlike the Cahn–Hilliard prediction the growth is not observed at a constant wavenumber. As is well-known, the thermal-noise Cook term causes the peak to slowly shift in right from the beginning. However, the magnitude of the shift seen in these data is too large to be simply accounted for by the effects of thermal noise. Our results imply that since the kinetics in the polymer solution is faster as compared to polymer blends, nonlinear terms are important right from the early stages. Similar results were reported by Wiltzius et al.[6] on the kinetics of a blend of protonated and deuterated polybutadiene. In their measurements,[6] although the very first data show some evidence for nonlinear effects, they found that an analysis of the initial growth rate, $R(k)$, was consistent with the CHC model.

In the following sections we analyze our data in three different time regimes, corresponding to the early, intermediate, and late stages of the phase-separation process.[5,12] In the early stages of spinodal decomposition, the time evolution of the concentration fluctuation, δc, is predicted by the linear Cahn–Hilliard theory to grow exponentially and the wavelength of the dominant mode is either constant or slowly growing if one allows for the thermal fluctuations as introduced by Cook.[9] In the intermediate stage both the wavelength of the dominant mode of fluctuations k_m and amplitude of the fluctuations δc grow with time. In the late stage, the amplitude of the concentration fluctuations δc reaches the equilibrium value of the concentration difference of the two coexisting phases, but the wavelength grows in a self-similar manner.[5,6] It should be noted that the transitions between these three stages are not necessarily sharply defined.

Early Time Behavior. As seen in Figure 2d the initial growth of the scattered intensity appears to be exponential for very early times ($t \leq 100$ s). This behavior is seen for both samples at all the different quenches. The time up to which this occurs increases with decreasing quench depth, decreasing k and increasing M. Following the approach used by several groups for polymer blends,[3,5,6] we use the linear Cahn–Hilliard model to determine the initial growth rate, i.e., $R(k)$ at $t = 0$. Strictly speaking, this linear theory is valid only when the growth is exponential and the position of the scattering maximum is unchanged in time (or slowly varying if one includes the thermal-noise term due to Cook). The latter condition is clearly not true for our data. However, the linear model may still be a good approximation for the initial growth rate, $R(k)$, at low k's, since (i) the effects of the Cook term are small when $k - k_m$ is large and (ii) the nonlinear terms that are responsible for the change of k_m with time arise from a coupling of fluctuations of different sizes and are thus likely to be more important in the vicinity of k_m where the magnitude of the fluctuations are much larger than those at $|k| \ll |k_m|$. Thus, such an analysis could be useful in estimating the characteristic length and time scale in the system. According to the linear Cahn–Hilliard theory, the scattered intensity is given as

$$I_s(k,t) \sim e^{2R(k)t} \tag{3}$$

where

$$R(k) = Dk^2\left(1 - \frac{k^2}{2k_m^2(0)}\right) \tag{4}$$

Decrease of the initial slope, $R(k)/k^2$, with increasing k^2 is clearly seen in Figure 2d. From semilog plots of scattered intensity versus k^2t (cf. Figure 2d), we get $R(k)/k^2 = D[1 - k^2/2k_m^2(0)]$. In order to determine D from this information, one needs an estimate of $k_m(0)$. According to CHC theory as discussed by Binder,[12] the relationship between $k_m(0)$, the correlation length, ξ^-, and the radius of gyration, R_g, is given by

$$k_m(0) = \frac{1}{\sqrt{2}}k_c = \frac{1}{\sqrt{2}}\frac{1}{\xi^-} \tag{5}$$

Here $0 < k < k_c$ represents the region of wavevectors where growth rate is positive, which means the fluctuations become amplified rather than decay. As described in Binder, $k_c = 1/\xi^-$, where ξ^- is the concentration correlation length below T_s. According to the Ising model, $\xi^- = \xi_0^-(T_s/T - 1)^{-2/3}$. The prefactor ξ_0^- is the amplitude of the correlation length, which is different for measurements above T_s versus below T_s. According to renormalization group calculations[24] ξ_0^-, the amplitude of the correlation length measured in the two-phase region, is related to the correlation length measured in the one-phase region, ξ_0^+, via $\xi_0^- = 0.524\xi_0^+$.

In order to determine ξ_0^+, we have used the relationship between correlation length and the radius of gyration in a dilute polymer solution, $\xi_0^+ = R_g/\sqrt{3}$. To determine R_g, we note that CH is a Θ solvent for PS. For PS at a temperature below Θ the polymer chain would be collapsed. Thus we also have to take into consideration the temperature dependence of the radius of gyration, $R_g(T)$, below the Θ temperature ($\Theta = 308.4$ K for PS in CH).

According to the prediction of the coil–globule transition,[25] R_g for $T < \Theta$ is given by

$$R_g(T) = \left(\frac{\Theta - T}{\Theta}\right)^{-1/3} N^{-1/6} R_g(\Theta) \tag{6}$$

Here N, the monomers in the polymer chain, is equal to $M_w/104$ for PS. The value of R_g at the Θ temperature is given by $R_g(\Theta) = aN^{1/2}$, ($a = 2.75$ Å[26] for PS). Taking everything into consideration, $R_g(T_s) = 110.5$ Å for sample 1 and $R_g(T_s) = 346.5$ Å for sample 2. Using this estimate,

Table I
Results of the Linear Cahn-Hilliard Analysis for Samples 1 and 2 for Different Quench Depths, ΔT[a]

ΔT, K	$D \times 10^{-10}$, cm^2 s^{-1}	$k_m(0) \times 10^4$, cm^{-1}	τ_0, s	α	β
		Sample 1			
0.45	3.83	2.79	3.35	0.49	1.1
0.55	4.66	3.19	2.11	0.47	1.0
0.65	5.35	3.56	1.47	0.51	1.0
0.75	5.73	3.92	1.14	0.43	1.2
0.95	7.84	4.59	0.61	0.53	1.2
		Sample 2			
0.25	0.87	0.59	330.2	0.59	b
0.40	1.86	0.81	81.94	0.59	1.0
0.75	3.78	1.23	17.48	0.54	1.0
1.25	6.12	1.73	5.46	0.47	1.0

[a] The exponent α was determined as the best effective fit to each of the data sets shown in Figure 3. The exponent β is only defined over a very limited range of times and thus represents an asymptotic value. [b] No region of power law growth could be identified.

we can obtain $k_m(0)$. We emphasize that the main purpose of this calculation is to get a characteristic length scale, and clearly there might be additional effects that depend weakly on the nature of the solvent and the monomer structure.

Thus the number of unknown parameters in eq 4 is reduced from two to one, and we can solve eq 4 to obtain D at different k values and obtain the average value. The results of this analysis are shown in Table I for both the samples. For both samples we observe that the characteristic time of the phase-separation process, $\tau_0 = 1/Dk_m(0)$,[2] increases while the characteristic wavenumber, $k_m(0)$, decreases as one approaches the spinodal temperature. As a consequence of this, for shallower quenches we are able to probe mostly the early and intermediate stages of the phase-separation process whereas for deeper quenches we are able to see the late stage. The dynamics is slower for the higher molecular weight, and this can be seen in the time that it takes for the contrast to develop to a detectable level. We observe that, for the same quench depth, $\Delta T = T_s - T$, $D \sim 2$ times smaller, and τ_0 is ~ 25 times larger for the higher molecular weight sample as compared to the lower molecular sample. We interpret this in terms of the molecular weight dependence of the polymer dynamics. Since the ratio of the molecular weights is ~ 12, these results are in better agreement with Zimm dynamics ($D \sim M_w^{-0.5}$ and $\tau_0 \sim M_w^{1.5}$) than with either Rouse or reptation dynamics.[27] The validity of Zimm dynamics for dilute solutions has been well established from dynamic light-scattering measurements of the self-diffusion coefficients in dilute solutions.[27] It is important to note that our observation of Zimm dynamics is obtained from the two-phase region and the D values correspond to the collective diffusion constant.

The diffusion constant decreases as T approaches T_s scaling as $D \sim (T_s - T)^{0.6}$. This result is in good agreement with the result obtained from measurements done *above* the critical point,[14] $D \sim (T - T_s)^{0.77}$, and with the prediction of the Ising model,[28] which gives $D \sim (T - T_s)^{0.67}$.

Our analysis shows that the linear Cahn-Hilliard model works reasonably for the extrapolated initial growth rate in the polymer solution case, in spite of the fact that the position of the maximum in the structure factor is changing from the earliest observation. The effects of including the thermal noise as done by Cook[9] and nonlinear terms as done in the Langer-Bar-on-Miller model[29] will be discussed in a future paper.

Intermediate- and Late-Stage Growth. As mentioned earlier, in the intermediate stage the concentration fluctuations grow in both amplitude and size while in the late stages only the size changes, the amplitude having reached the equilibrium composition difference. These two stages also differ in the relative thickness of the interface, which is larger and more diffuse in the intermediate regime and becomes smooth and narrower in the late stages. The growth of the phase-separating structure is expected to obey power-law scaling in the late stages, with $k_m \sim t^{-\alpha}$ and $I_m \sim t^{\beta}$. Here k_m denotes the position of the peak maximum and I_m the intensity at the maximum. The exponents α and β obey the hyperscaling relation $\beta = 3\alpha$ for late-stage growth in three dimensions.[1]

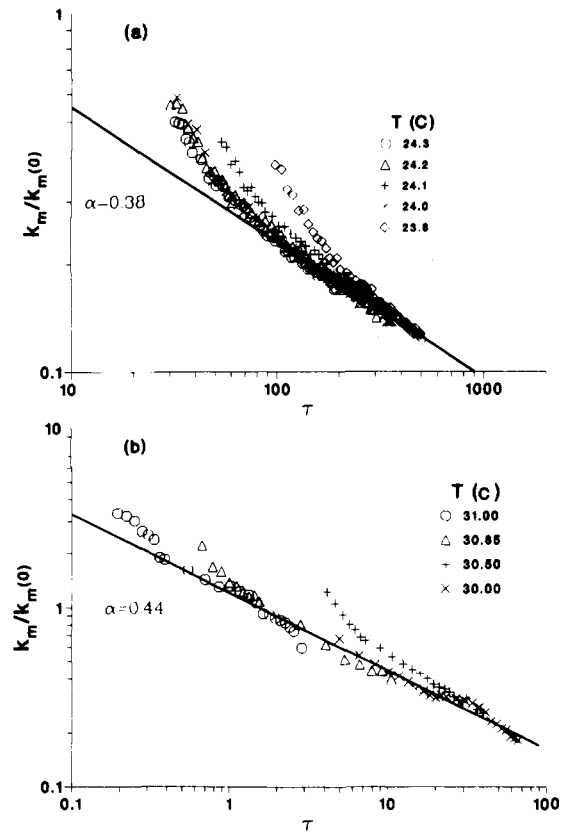

Figure 3. Position of the maximum in the scattered intensity, $k_m/k_m(0)$ as a function of time, τ, in reduced units (see text). The results for all the different quench temperatures are shown (a) for sample 1 and (b) for sample 2. The asymptotic power law regime is drawn as a solid line.

The linear analysis of the initial growth rate provides us with an estimate of the characteristic length and time scales. Using these values, we plot the peak position, k_m (in units of $k_m(0)$), and the intensity at the maximum, I_m, as a function of the reduced time $\tau = t/\tau_0$, for the different quenches for both the samples (Figures 3 and 4). As shown in Table I, α ranges from 0.4 to 0.5. Unlike the work with polymer blends, we never observed a value of $\alpha = 1/3$, suggesting that hydrodynamic effects are important at all stages of the spinodal decomposition process in the dilute solution case. Several different droplet growth and coarsening mechanisms predict a value of $\alpha = 1/3$. For example, the evaporation-condensation mechanism of Lifshitz and Slyozov,[30] the droplet coalescence growth mechanism of Binder and Stauffer,[31] and the coarsening of solid interfaces all predict $\alpha = 1/3$. Values of $\alpha > 1/3$ are obtained if one includes hydrodynamic effects.[32] The model of Siggia,[33] where convective flow with hydrodynamic interactions are dominant, gives $\alpha = 1$.

According to the dynamic scaling hypothesis, the late-stage data plotted in reduced units should be independent of the quench depth. We observe only a partial collapse

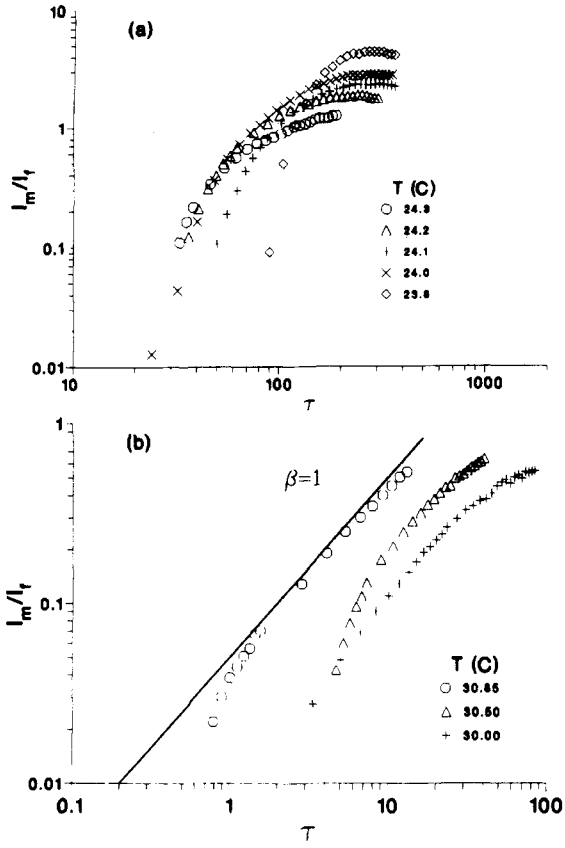

Figure 4. Maximum scattered intensity, I_m, obtained at various quench temperatures as function of time in reduced units. (a) The data for sample 1 showing rapid initial growth followed by a region of slower growth. It is clear that no extensive power law growth regime can be identified; however, there appears to be a transition at late stages to power law growth with $\beta \sim 1$. The time at which this transition to late-stage growth occurs depends on quench depth occurring earlier in reduced time for deeper quenches. (b) The same analysis for sample 2 suggests that most of the data are in the early and intermediate stages. An asymptotic power law growth with $\beta = 1$ (see text) can be seen. The line of slope 1 is drawn to guide the eye.

of the data (Figure 3), suggesting that most of it lies in the intermediate stage of the phase-separation process. An examination of parts a and b of Figure 3 shows that the transition from the intermediate to the late stage depends on quench depth, the deeper quenches showing more of the late stages, since the process happens on a faster real time scale for T further away from T_s.

In the late stages of spinodal decomposition in a critical sample of polymer blends, an exponent of $\alpha \simeq 1/3$ has been observed[5,6] whereas in the intermediate stages the exponent was found to be dependent on the quench depth. We observe similar behavior for the lower molecular weight solution, with α becoming independent of quench depth for $\tau > 100$. An additional difference is that, for $\tau < 100$ (i.e., in the intermediate stage), $\alpha > 1/3$, in contrast to the results with polymer blends where it is less than $1/3$. Similar results are seen in the higher molecular weight sample. To rule out experimental artifacts, we used our apparatus under identical optical conditions to measure spinodal decomposition in the isobutyric acid–water system where the peak positions are in the same range as those in our samples. For a critical quench close to T_s, we found that α was $1/3$, in agreement with the results of Wong and Knobler.[21]

Having ruled out experimental artifacts, we suggest two possible explanations for this somewhat intriguing observation of a larger value of α at earlier times. Since $\alpha > 1/3$ is indicative of hydrodynamic interactions, our finding that α decreases with increasing time and asymptotically approaches a value between 0.4 and 0.5 implies that hydrodynamic effects are more important at earlier times than at later times. This may be happening because the initial concentration of the solution is in the dilute regime where hydrodynamic interactions are not screened out and the polymer dynamics is described by Zimm model. However, as phase-separation proceeds most of the polymer molecules are in the concentrated or semidilute regions where hydrodynamic screening is quite effective. Thus with increasing time, hydrodynamic effects become less important, in stark contrast to the situation with binary fluids where hydrodynamic effects become more important in the late stages. If this argument is correct, then α should be close to $1/3$ at earlier times in the spinodal decomposition of concentrated polymer solutions as compared to that of a dilute solution of the same molecular weight. Preliminary results on a high-concentration solution of PS–CH tend to support this.

An alternative explanation is that in the case of the polymer solution the mobility is a strong function of polymer concentration and changes with time as the phase-separation proceeds. Thus the characteristic time scale itself varies during the phase-separation process, becoming longer as the phase separation proceeds. At present no theoretical model deals with the case where the mobility and characteristic time scale are themselves time dependent.

Parts a and b of Figure 4 show a log–log plot of intensity at the peak I_m/I_f versus reduced time τ for samples 1 and 2. For both samples 1 and 2 we observe the slope β to be continuously changing, approaching an asymptotic behavior with a slope β close to 1 ($\tau > 60$ and 6, for samples 1 and 2, respectively). The initial growth is more rapid, being exponential instead of power law, suggesting that at early times the dominant contribution to the amplitude of the fluctuations is from the linear terms even though the growth of wavelength, k_m, of the dominant mode of fluctuations is influenced by the nonlinear terms. Since the width of the coexistence curve is broader for deeper quenches, the equilibrium value of the amplitude of the concentration fluctuations, δc, reached in the late time should increase with increasing quench depth. This is well borne out by our data for sample 1 as seen in the increase of the asymptotic value of I_m/I_f with quench depth. For sample 2 this is not seen, again indicating that most of the measured data are in the intermediate stage where the amplitude has not yet reached the equilibrium value.

During the late stages where no further concentration changes occur in the demixed phases, scaling theory predicts $\beta = 3\alpha$. The time range explored in our data never seems to quite approach this as seen in Table I. This further corroborates our conclusion that most of our measured data fell in the intermediate region. It was not possible to extend the measurements to later times because the peak position had become so low as to be obscured by the transmitted beam. It should also be pointed out that intensity measurements are susceptible to greater inaccuracy than measurements of the peak position since small effects of multiple scattering and background subtraction can still occur even though we have tried to minimize these effects as discussed earlier.

Dynamic Scaling of the Structure Factor. At late times, according to the dynamic scaling hypothesis,[1] the structure factor $S(k,t)$ can be written in terms of a time-

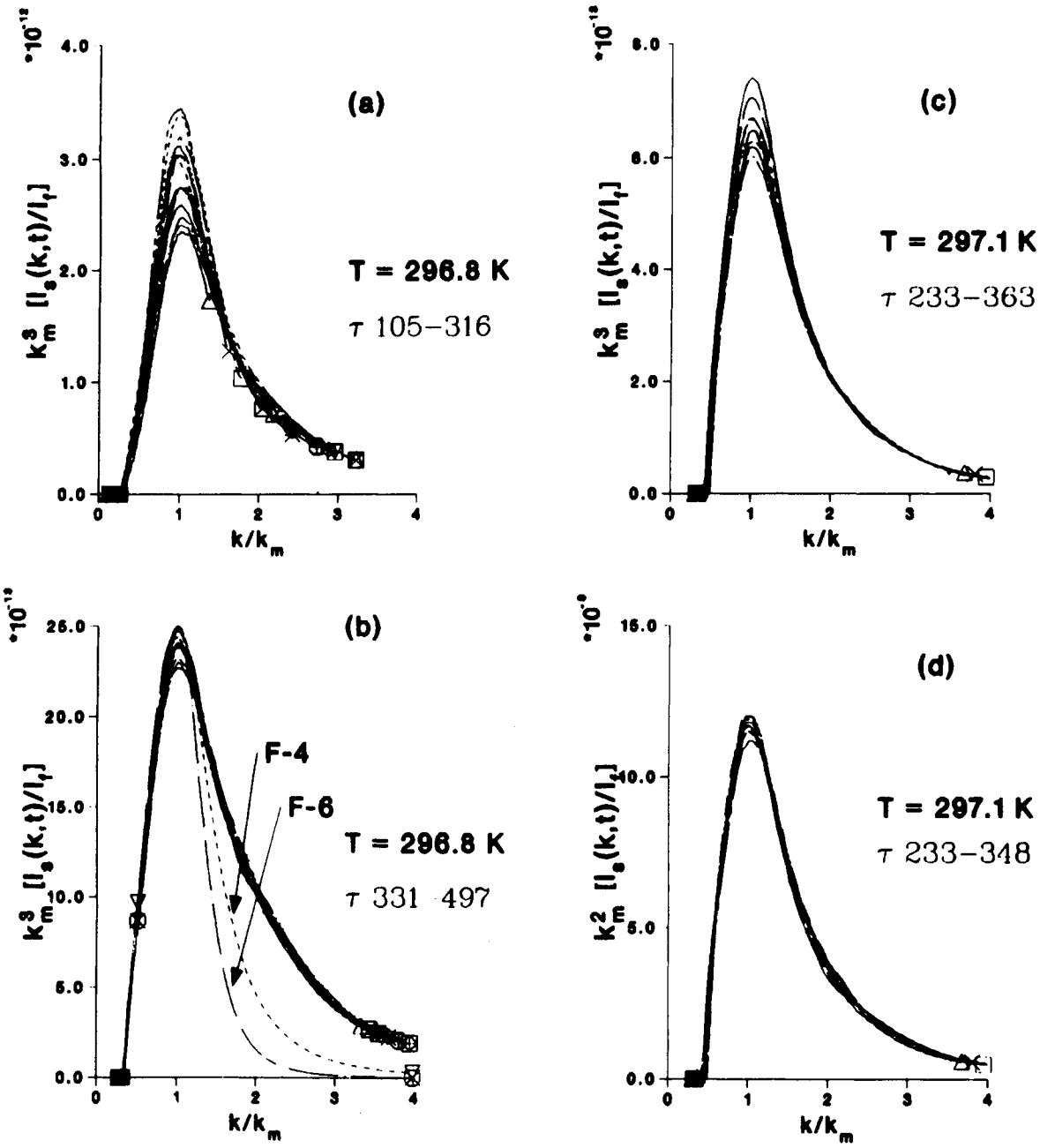

Figure 5. Scaled scattering functions for sample 1. (a) Early- and intermediate-stage data ($\tau < 316$) for a deep quench $T_q = 296.8$ K, showing no collapse. (b) For the same quench as in (a) the data collapse for $\tau > 331$, which is indicative of late time scaling regime. Also plotted are the theoretical scaling functions of Furukawa for off-critical and critical quenches, identified as F-4 and F-6, respectively (see text for definition). (c) Data for the shallow quench, $T_q = 297.1$ K plotted using eq 7 with $d = 3$. (d) The same data as in (c) plotted with $d = 2$ in eq 7.

independent scaling function, $F(k/k_m(t))$

$$k_m{}^d S(k,t) = F(k/k_m(t)) \tag{7}$$

where d is the spatial dimension of the system. Since the scattered intensity is proportional to the structure factor, the applicability of this scaling can be tested by plotting $k_m{}^3 I_s(k,t)/I_f$ versus k/k_m for different times. Figure 5 shows the results of such an analysis for sample 1 for two different quench temperatures. For the case of a deep quench, $T_q = 296.8$ K, we find that at early times ($\tau < 316$) the data do not collapse (Figure 5a) whereas at late times ($\tau > 331$) the data collapse, indicating that dynamic scaling is satisfied at later stages but not in the intermediate stages. For a shallow quench $T_q = 297.1$ K, the data do not collapse for even the latest times at which measurements could be made. These results are consistent with the interpretation given earlier, that the slower time scale and larger characteristic length scale lead to most of the data falling in the intermediate time scale for shallow quenches. Similar results were observed for the higher molecular weight sample 2, where true late-stage behavior could never be detected.

We tried an empirical approach to examine the question of whether any alternative form of scaling exists in the intermediate region. We found that if we allowed d in eq 7 to vary with the quench depth and the time regime, then it was possible to scale the data in the intermediate regime.[34] Figure 5d shows that for $T_q = 297.1$ K the data collapse with $d = 2.0$. Similar results were obtained for the intermediate-stage data at other temperatures and also for the higher molecular weight sample. The value of d ranged between 1.7 and 2.5.

Since the term $(k_m)^d$ in the dynamic scaling equation (eq 7) arises from the dependence of the structure factor

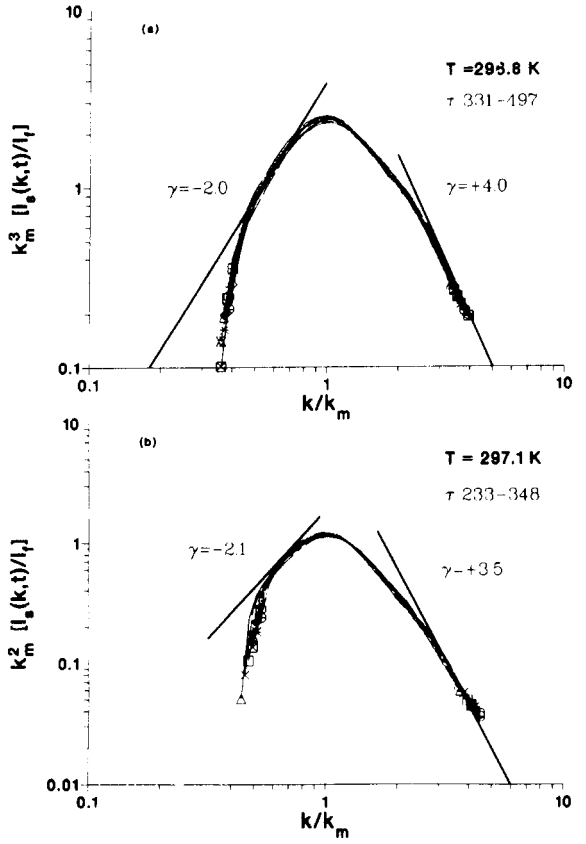

Figure 6. The asymptotic behavior of the scaled structure factor $F(k/k_m)$ for sample 1. (a) For a deep quench, T_q = 296.8 K, the same data as in Figure 6b shown on a log–log plot. Note that the slope $\gamma = -2$ for $k/k_m < 1$ and equals 4 for $k/k_m > 1$. (b) For a shallow quench, T_q = 297.1 K, the data of Figure 6d shown on a log–log plot. Note that $\gamma = -2.1$ for $k/k_m < 1$ but equals 3.5 for $k/k_m > 1$. Note also that, although the collapse of the data for different times occurs only with $d = 2.0$, the asymptotic power law behavior in k has the same exponent irrespective of the value of d in eq 7, because the factor k_m^d becomes an additive constant in a log–log plot.

on the volume of the scatterer, our result may be indicative of scattering from "rough" domains in the intermediate stages, possibly arising from the very diffuse and relatively large interface that exists in the intermediate stages as compared to the late stages. The k dependence of the structure factor is also suggestive of scattering from a diffuse interface as discussed below.

According to Furukawa,[35] the asymptotic scaled structure factor, $F(k/k_m)$, scales as $(k/k_m)^{-\gamma}$, where $\gamma = -2$ for for $k/k_m < 1$ and $\gamma = 4$ or 6 for $k/k_m > 1$. The value of $\gamma = 4$ implies the existence of isolated phase-separated clusters and is expected for off-critical quenches whereas $\gamma = 6$ implies a percolating structure and is expected for critical quenches. It is perhaps interesting to see if any effective power law behavior can be discerned from the structure factor data obtained here. Since the range of k-space accessible in these measurements is limited, we recognize that the conclusions of such an analysis are at best indicative of effective exponents. However, such analysis has often been done in polymer blends over approximately similar ranges of k. Thus we attempt similar analysis of our data but caution against taking the exponents too literally.

As shown in parts and and b of Figure 6 for the low molecular weight sample, the exponent $\gamma = -2$ for $k/k_m < 1$ is obtained for both deep and shallow quenches. However, for $k/k_m > 1$, the exponent $\gamma = 4$ for deep quenches and $\gamma \simeq 3.5$ for shallow quenches. Similar analysis for polymer blends by several authors gives values of $\gamma = 4$, with $\gamma = 6$ observed in two cases.[5,36] The values of γ obtained by us would suggest that, in the case of deep quenches, where late stages of spinodal decomposition are reached, the clusters are isolated and have a smooth interface, which gives the characteristic Porod scattering.[36] Since this sample was almost critical, we should have obtained $\gamma = 6$ according to the Furukawa theory. As discussed in the recent review by Binder,[12] disagreements with the Furukawa theory also show up in other experiments[6] and in computer simulations where also one obtains $\gamma = 4$ instead of 6 for critical quenches. For the shallow quench case where the laste measurements are in the intermediate stages, we get $\gamma = 3.5$, which is not too far from the value of $\gamma = 4$. Values of γ slightly less than 4 were obtained by the numerical solution work of Chakrabarti et al.[37] for the polymer blend case. The value of $\gamma = 3.5$ may indicate that in the intermediate stages of spinodal decomposition in polymer solutions the morphology is still diffuse and the interface rough. With increasing time the interface becomes less diffuse and γ increases toward the Porod value of 4. Since the range of k values explored in the present SALS experiment is very limited, our analysis can only be regarded as an indication of an effective power law and clearly suggests that a further study over bigger k ranges might be very useful.

As a final comparison of the late-stage structure factor with the Furukawa prediction, Figure 5b shows the predicted functional form $F(x) = 3x^2/(2 + x^6)$ and $4x^2/(3 + x^8)$, for off-critical and critical quenches, respectively ($x = k/k_m$). These are identified as F-4 and F-6, respectively, in the figure. A comparison of the predicted function with the measured scaled structure factor shows good agreement for $k/k_m < 1$ and a clear disparity for high values of k/k_m. In this region, even though the asymptotic behavior is given by the exponent $\gamma = 4$, the actual function does not match. The mismatch is most pronounced in the vicinity of $k/k_m \simeq 2$, suggesting that perhaps there is a secondary peak in this region. Recent experiments[6] and theoretical models[38] have suggested the existence of a second peak at $k/k_m = 2$. This is also supported by the work of Chakrabarti et al.,[37] who obtained the time evolution of the structure factor by numerically integrating the spinodal decomposition equations for polymer blends based on the Flory–Huggins–de Gennes free-energy functional and found no agreement with either of Furukawa's functional forms.

Conclusions

To summarize, we have measured the spinodal decomposition kinetics in polystyrene–cyclohexane solutions of two different molecular weights for several different quench temperatures. As expected, the kinetics is slower for the high molecular weight sample. While most of the measurements accessible by small-angle light scattering fall in the intermediate to late stages, the earliest data show some features that are indicative of a linear CHC model. Although the contribution of nonlinear terms is probably important from the beginning, it is perhaps reasonable to analyze the initial growth rate in terms of the linear theory. Such an analysis was used to determine the initial diffusion constant, and the molecular weight dependence shows that the dynamics is consistent with the predictions of the Zimm model.

Intermediate- and late-stage growth appear to be described by power law relations. The exponents become independent of quench depth only in the late stages, and this could only be reached for the lower molecular weight

sample for deep quenches. The characteristic time scale was slower and the characteristic length scale bigger for both shallow quenches and higher molecular weights. As a consequence, it was not possible to measure the scattering in truly late stages in these cases.

The late-stage structure factor could be scaled into a universal time-independent form in agreement with the predictions of the dynamic scaling hypothesis. However, in the intermediate stages such a collapse of the data could only be obtained by modifying the dynamic scaling equation to allow the dimension d to vary with quench depth and time. Although this is clearly an empirical procedure, we tentatively suggest that this may be related to the structure of the interface in the intermediate stages. The asymptotic behavior of the scaled structure factor was also found to be anomalous in the intermediate stages. The results are suggestive of a diffuse interface in this time range.

A detailed comparison with the predictions of the Furukawa model was made. The results showed that the structure factor scales according to the Furukawa prediction for $k < k_m$ but that for $k > k_m$ the exponent $\gamma = 4$ even though we considered a critical quench. The actual functional form proposed by Furukawa agrees on the low k side but is quite inadequate on the high k side. Some evidence for a second peak at $k/k_m \simeq 2$ can be seen in the data.

In conclusion, we note that while some of the results obtained here for the polymer solution case are similar to those seen in blends, many differences can also be seen. For the polymer solution most of the data accessible to small-angle light scattering fall in the intermediate time scale where there is no existing theoretical model. It is clear that a proper theoretical treatment, which takes into account the effects of phase-diagram asymmetry and concentration-dependent mobility of polymer solutions and also includes nonlinear effects, is needed in order to get a detailed quantitative agreement between theory and experiment.

Acknowledgment. We thank Profs. Bill Klein and Karl Ludwig of Boston University for many helpful discussions and acknowledge the technical assistance of Jeyandran Abraham throughout the whole project. This research was supported by a grant from the NSF.

References and Notes

(1) Gunton, J. D.; San Miguel, M.; Sahni, P. S. In *Phase Transitions and Critical Phenomena*; Domb, D., Lebowitz, J. L., Eds.; Academic Press: London, 1983; Vol. 8, p 267.
(2) Snyder, H. L.; Meakin, P. *J. Chem. Phys.* **1983**, *79*, 5588.
(3) Sato, T.; Han, C. C. *J. Chem. Phys.* **1988**, *88*, 2057. Okada, M.; Han, C. C. *J. Chem. Phys.* **1986**, *85*, 5317.
(4) Nishi, T.; Wang, T. T.; Kwei, T. K. *Macromolecules* **1975**, *8*, 227.
(5) Hashimoto, T.; Itakura, M.; Hasegawa, H. *J. Chem. Phys.* **1986**, *85*, 6118. Hashimoto, T.; Itakura, M.; Shimidzu, N. *J. Chem. Phys.* **1986**, *85*, 6773. For a recent review, see: Hashimoto, T. In *Phase Transitions*; Gordon and Breach Science Publishers Inc.: New York, 1988; Vol. 12, pp 42–119.
(6) Wiltzius, P.; Bates, F. S.; Heffner, W. R. *Phys. Ref. Lett.* **1988**, *60*, 1538. Bates, F. S.; Wiltzius, P. *J. Chem. Phys.* **1989**, *91*, 3258.
(7) Nose, T. In *Space-Time Organization in Macromolecular Fluids*; Tanaka, F., Doi, M., Ohta, T., Eds.; Springer-Verlag: New York, Berlin, and Heidelberg, 1989; Vol. 51, p 40. Earlier work is reviewed in: Nose, T. *Phase Transitions* **1987**, *8*, 245.
(8) Cahn, J. W.; Hilliard, J. H. *J. Chem. Phys.* **1958**, *28*, 258.
(9) Cook, H. E. *Acta Metall.* **1970**, *18*, 297.
(10) de Gennes, P.-G. *J. Chem. Phys.* **1980**, *72*, 4756.
(11) Pincus, P. *J. Chem. Plys.* **1981**, *75*, 1996.
(12) Binder, K. *J. Chem. Phys.* **1983**, *79*, 6385. For a recent review, see: Binder, K. In *Materials Science and Technology: Phase Transformation in Materials*; Haasen, P., Ed.; VCH Verlagsgesellschaft: Weinheim, Germany, 1990; Vol. 5, p 1.
(13) Van Aarsten, J. J.; Smolders, C. A. *Eur. Polym. J.* **1970**, *6*, 1105.
(14) Kuwahara, N.; Fenby, D. V.; Tamsky, M.; Chu, B. *J. Chem. Phys.* **1971**, *55*, 1140.
(15) Nakata, M.; Kuwahara, N.; Kaneko, M. *J. Chem. Phys.* **1975**, *62*, 4278.
(16) Kojima, J.; Kuwahara, N.; Kaneko, M. *J. Chem. Phys.* **1975**, *63*, 333.
(17) Nakata, M.; Dobashi, T.; Kuwahara, N.; Kaneko, M. *Phys. Rev. A.* **1978**, *18*, 2603.
(18) des Cloizeaux, J.; Jannink, G. *Les Polymeres en solution: leur Modelisation et leur Structure*, Les editions de physique, 1987.
(19) Perzynski, R.; Delsanti, M.; Adam, M. *J. Phys.* **1987**, *48*, 115.
(20) Goldburg, W. W. In *Scattering Techniques Applied to Supramolecular and Nonequilibrium Systems*; Chen, S. H., Chu, B., Nossal, R., Eds.; Plenum Press: New York, 1980; and references therein.
(21) Wong, N. C.; Knobler, C. M. *J. Chem. Phys.* **1978**, *69*, 725.
(22) Chu, B.; Schoenes, F. J.; Fisher, M. E. *Phys. Ref.* **1969**, *185*, 219.
(23) Pine, D. J. *Rev. Sci. Instrum.* **1984**, *55*, 856.
(24) Guenoun, P.; Gastaud, R.; Perrot, F.; Beysens, D. *Phys. Rev. A.* **1987**, *36*, 4876.
(25) Park, I. H.; Wang, Q. W.; Chu, B. *Macromolecules* **1987**, *20*, 1965.
(26) Cotton, J. P.; Decker, D.; Benoit, H.; Farnoux, B.; Higgins, J.; Jannink, G.; Ober, R.; Picot, C.; des Cloizeaux, J. *Macromolecules* **1974**, *7*, 863.
(27) Doi, M.; Edwards, S. F. *The Theory of Polymer Dynamics*; Clarendon Press: Oxford, 1986.
(28) Stanley, H. E. *Introduction to Phase Transitions and Critical Phenomena*; Oxford University Press: Oxford, 1971.
(29) Langer, J. S.; Bar-on, M.; Miller, H. D. *Phys. Rev. A* **1975**, *11*, 1417.
(30) Lifshitz, I. M.; Slyozov, V. V. *J. Phys. Chem. Solids* **1961**, *19*, 35.
(31) Binder, K.; Stauffer, D. *Phys. Rev. Lett.* **1974**, *33*, 1006.
(32) Kawasaki, K. *Prog. Theor. Phys.* **1977**, *57*, 826.
(33) Siggia, E. D. *Phys. Rev. A.* **1979**, *20*, 595.
(34) Bansil, R.; Lal, J. In *Extended Abstracts: Fractal Aspects of Materials: Disordered Systems*; Weitz, D. A., Sanders, L. M., Mandelbrot, B. B., Eds.; Materials Research Society: Pittsburgh, PA, 1988; EA-17, p 255. Lal, J.; Bansil, R. In *Fractal Aspects of Materials 1989*; Kaufman, J. H., Martin, J. E., Schmidt, P. W., Eds.; MRS: Pittsburgh, PA, 1989; EA-20, p 11.
(35) Furukawa, H. *Phys. A.* **1984**, *123*, 497.
(36) Tomlins, P. E.; Higgins, J. S. *J. Chem. Phys.* **1989**, *90*, 6691.
(37) Chakrabarti, A.; Toral, R.; Gunton, J. D.; Muthukumar, M. *J. Chem. Phys.* **1990**, *92*, 6899.
(38) Ohta, T.; Nozaki, H. In *Space-Time Organization in Macromolecular Fluids*; Tanaka, F., Doi, M., Ohta, T., Eds.; Springer-Verlag: New York, Berlin, and Heidelberg, 1989; Vol. 51, p 51.

Registry No. PS, 9003-53-6.